

Fermion Condensate as Higgs substitute

G. Cynolter and E. Lendvai

Theoretical Physics Research Group of Hungarian Academy of Sciences, Eötvös University, Budapest, 1117 Pázmány Péter sétány 1/A, Hungary

Abstract

We propose and analyze an alternative model of dynamical electroweak symmetry breaking. In the Standard Model of electroweak interactions the elementary Higgs field and the Higgs sector are replaced by vector-like fermions and their interactions. The new fermions are a weak doublet and a singlet. They have kinetic terms with covariant derivatives and gauge invariant four-fermion interactions. The model is a low energy effective one with a natural cutoff in the TeV regime. Due to the quartic fermion couplings the new fermions form condensates. The new fermions mix in one condensate and the mixing breaks the electroweak symmetry. The condensates contribute to the masses of the new fermions, which may or may not have mass terms in the original Lagrangian. Gap equations are derived for the masses of the new fermions and the conditions are presented for mass generations and electroweak symmetry breaking. In the spectrum there are two neutral fermions and a charged one with mass between the neutral ones. The new sector can be described by three parameters, these are the two neutral masses and the mixing angle. These parameters are further constrained by the unitarity of two particle scattering amplitudes, providing an upper bound for the lighter neutral mass depending on the cutoff of the model. The standard chiral fermions get their masses via interactions with the condensing new fermions, but there is no mixing between the standard and the new fermions. There is an effective composite scalar in the model at low energies, producing the weak gauge boson masses in effective interactions. The ρ parameter is one at leading order. The model can be constrained by one-loop oblique corrections. The Peskin-Takeuchi S and T parameters are calculated in the model. The parameters of the model are only slightly constrained, the T parameter requires the new neutral fermion masses not to be very far from each other, allowing higher mass difference for higher masses and smaller mixing. The S parameter gives practically no constraints on the masses. The new fermions can give positive contributions to T allowing for a heavy Higgs in the precision electroweak tests. It is shown that the new fermions will be copiously produced at the next generation of linear colliders and cross sections are presented

for the Large Hadron Collider. An additional nice feature of the model is that the lightest new neutral fermion is an ideal and natural dark matter candidate.

1 Introduction

The Standard Model of particle physics successfully describes known collider experiments reaching the permille level in case of some observables. The only missing particle of the Standard Model is the elementary Higgs boson. In the minimal Standard Model a weak doublet (hypercharge $Y=1$) scalar field is postulated with an *ad hoc* scalar potential to trigger electroweak symmetry breaking. This provides a very economical and simple description. Three Goldstone Bosons are eaten up by the W^\pm , Z gauge bosons providing their correct masses, but the remaining single CP-even neutral Higgs scalar has evaded the experimental discovery so far. There exist experimental constraints on the mass of the Higgs boson. The LEP2 experiment has put a lower bound $M_H > 114.4$ GeV [1] and there is an exclusion window from the combined D0 and CDF measurements at the Tevatron [2] between 158 and 175 GeV. The precision data favour a light Higgs with a central value below the direct LEP2 bound. Including the results of the direct searches both at LEP2 and the Tevatron the upper limit is driven to $M_H \leq 147$ at 95 % C.L. from electroweak precision tests [1]. The Gfitter group has arrived at similar upper bounds $M_H \leq 159$ GeV (155 GeV) with or without the information of the direct Higgs searches [3].

Beside the missing experimental discovery, theories with elementary scalars are burdened with theoretical problems, like triviality and the most severe gauge hierarchy problem. Elementary scalars are unstable against radiative corrections and without fine tuning the Standard Model must be cut off at few TeV.

There are mainly two ways to solve these problems in particle physics, either impose new symmetries to protect the scalars or eliminate elementary scalars from the theory.

Supersymmetry is the number one candidate for beyond the Standard Model physics, it protects the quadratically unstable Higgs mass, the contribution of the superpartners cancel each other. The Minimal Supersymmetric Standard Model is very attractive considering that electroweak symmetry breaking is triggered radiatively, there are ideal dark matter candidates and gauge couplings unify better in supersymmetric Grand Unified Theories than in standard GUTs. However supersymmetric theories involve a huge parameter space, all known particles are doubled and no satisfactory mechanism has been worked out for supersymmetry breaking. None of the predicted new superpartners have been found in any of the experiments and supersymmetry may start to lose it's appeal. Another shortcoming is that with no discovery the superpartner masses and the scale of supersymmetry breaking are pushed higher and higher reformulating the fine tuning problem at a percent level.

There are strong indications, expectations and a “no lose theorem” that the LHC will reveal the physics of electroweak symmetry breaking. Either the LHC will find one or more Higgs bosons, it could be the Standard Model one or a scalar coming from an extended Higgs sector like the MSSM or the LHC will discover some sign of new, possibly strong dynamics that unitarizes the scattering of longitudinal gauge bosons in the TeV regime.

These observations motivate to study alternative models of electroweak symmetry breaking without elementary scalars.

The other main solution to the hierarchy problem employs the mechanism of dynamical symmetry breaking. The original technicolor idea [4, 5, 6] of fermion condensation is already more than thirty years old, it is based on real phenomena of QCD. Technicolor still gives motivation for new research, see a recent review [7], Chivukula et al. in [1] and references therein. New chiral fermions are postulated which are charged under the new technicolor gauge group, the new interaction becomes strong condensing the techni-fermions charged under the weak $SU_L(2)$. To provide fermion masses extended technicolor gauge interactions (ETC) [8, 9] must be included. The tension between sizeable quark masses and avoiding flavor changing neutral currents led to introduce walking, near conformal dynamics [10, 11]. These ideas and the phase diagram of strongly interacting models triggered activity in lattice studies [12], and further new technicolor models were constructed based on adjoint or two index symmetric representations of the new fermions [13]. The heavy top quark is natural in top condensate models [14, 15], and there are extra dimensional realizations, too [16, 17].

Inspired by discretized higher dimensional theories "little Higgs" [18] models provide a new class of composite Higgs models, and they attracted considerable interest solving the "little hierarchy problem" [19] allowing to raise the cutoff of the theory up to 10 TeV without excessive fine tuning [20, 21]. Little Higgs models realize the old idea that the Higgs is a pseudo Goldstone boson of some spontaneously broken global symmetry [22]. Contrary to supersymmetric models divergent fermion (boson) loops cancel fermion (boson) loops. Little Higgs models still require large fine tuning unless they possess custodial symmetry at the price of highly extended gauge groups. There are various models where the Higgs is composite [23], the idea was recently realized in extra dimensions [24]. Higgsless models [25] do not utilize a scalar Higgs boson, but using the AdS/CFT correspondence these are extra dimensional "duals" of walking technicolor theories.

In this chapter we present a recently proposed alternative symmetry breaking model of electroweak interactions [26]. The complete symmetry breaking sector is built from a new doublet and a singlet vector-like fermions, the Higgs is a composite state of the new fermions. Using vector-like fermions is advantageous compared to chiral ones as the constraints from precision electroweak measurements are much weaker. Vector-like fermions appear in several extensions of the Standard Model. They are present in extra dimensional models with bulk fermions e.g [27], in little Higgs theories [18, 20, 21], in models of so called improved naturalness consistent with a heavy Higgs scalar [28], in simple fermionic models of dark matter [29, 30], in dynamical models of supersymmetry breaking using gauge mediation, topcolor models [31]. Vector-like fermions were essential ingredients of our proposal, in which a nontrivial condensate of new vector-like fermions breaks the electroweak symmetry and provides masses for the standard particles [26].

In the Fermion Condensate Model the Higgs sector is replaced by the interactions of a new doublet $\Psi_D = \begin{pmatrix} \Psi_D^+ \\ \Psi_D^0 \end{pmatrix}$ and a singlet Ψ_S hypercharge 1 vector-like (non-chiral) fermion field. After electroweak symmetry breaking Ψ_D^+ field corresponds to a positively charged

particle and Ψ_D^0 to a neutral one. The new fermions are postulated to have effective non-renormalizable four-fermion interactions and the model is a low energy effective one, valid up to some intrinsic, physical cutoff, that is not be taken to infinity. Therefore we are not forced to add additional terms to calculate at lowest orders following [32], including extra terms will define a different model. The ultraviolet completion of the model is not yet specified, but as usual the four-fermion terms are expected to originate from some spontaneously broken gauge interactions. The key point is that the four-fermion interactions become strong at low energies and generate condensates of the new fermions including a mixed condensate of Ψ_D and $\bar{\Psi}_S$, $\langle \bar{\Psi}_S \Psi_D \rangle_0 \neq 0$. Gap equations are derived for the condensates and the condition of symmetry breaking is determined. The new fermions get contributions to their masses from the condensates. The vacuum solution of the model has a nontrivial weak $SU_L(2)$ quantum number and it spontaneously breaks the electroweak symmetry in a dynamical way. This symmetry breaking scheme was already utilized in our earlier works [33, 34]. The nontrivial condensate further generates mixing between the neutral component of the doublet and the singlet. The Ψ_D doublet has a standard kinetic terms with the usual covariant derivative and after the mixing the weak gauge bosons (W^\pm , Z) get their masses from the symmetry breaking condensate. The proposed model contains three new particles, two neutral and a charged fermions. The solution of the gap equations shows that the mass of the charged fermion is between the two neutral ones. The lighter neutral particle is an ideal dark matter candidate. The most important constraints on the parameters of the model are coming from the solution of the gap equation and the requirement of perturbative unitarity in two particle elastic scattering processes. Generally the new charged fermion tends to be nearly degenerate with the heavier neutral one. Perturbative unitarity sets an upper bound on the lighter neutral fermion depending on the range of validity of the model (the cutoff), it is $M_1 \leq 230$ GeV for $\Lambda = 3$ TeV.

Any beyond the Standard Model physics must face the tremendous success of the Standard Model in high energy experiments, it must have evaded direct detection and fulfill the electroweak precision tests. LEP1 and LEP2 measurements have set a direct lower bound [1] for a heavy charged strongly not interacting fermion (lepton) $M_+ > 100$ GeV and without assumptions $M_0 > 45$ GeV for neutral one. Oblique radiative correction which proved to be fatal in case of the original technicolor models are nearly harmless. The starting vector-like doublet and singlet gives no contribution to the Peskin-Takeuchi S and T oblique parameters [35] and the deviations are always proportional to the mixing among the new neutral fermions. Small enough but nonvanishing mixing will break the electroweak symmetry but gives small S and T . Finally the symmetry breaking solutions of the gap equations are so specially constrained that lead to a miniscule S and T parameters.

The rest of the chapter is organized as follows. In section 2 we present the proposed dynamical symmetry breaking model, then the gap equations are derived and solved, the solutions are further constrained by perturbative unitarity in section 4. In section 5 the interactions relevant in phenomenology and direct constraints from the LEP experiment are calculated. In section 6 we calculate the oblique electroweak parameters and section 7 contains the numerical results and figures. The cross sections for the LHC and the next generation of linear colliders are presented before the conclusion, and one appendix flashes

a new regularization method developed and used by us during this work.

2 The Fermion Condensate Model

Recently self-interacting vector-like fermions were introduced [26] in the Standard Model instead of an elementary standard scalar Higgs. The new colourless Dirac fermions are an extra neutral weak $SU(2)$ singlet ($T = Y = 0$) and a doublet

$$\Psi_S, \quad \Psi_D = \begin{pmatrix} \Psi_D^+ \\ \Psi_D^0 \end{pmatrix}, \quad (1)$$

with hypercharge 1. Similar fermions are often dubbed leptons, because they do not participate in strong interactions, and widely studied in the literature as we discussed in the introduction. A model with similar fermion content were studied by Maekawa [36, 37]. There is a new Z_2 symmetry acting only on the new fermions, which protects them from mixings with the standard model quarks and leptons, the new fermions may interact only in pairs. The lightest new fermion is stable providing an ideal weakly interacting dark matter candidate.

The new Lagrangian with gauge invariant kinetic terms and invariant 4-fermion interactions of the new fermions is L_Ψ ,

$$\begin{aligned} L_\Psi = & i\bar{\Psi}_D D_\mu \gamma^\mu \Psi_D + i\bar{\Psi}_S \partial_\mu \gamma^\mu \Psi_S - m_{0D} \bar{\Psi}_D \Psi_D - m_{0S} \bar{\Psi}_S \Psi_S + \\ & + \lambda_1 (\bar{\Psi}_D \Psi_D)^2 + \lambda_2 (\bar{\Psi}_S \Psi_S)^2 + 2\lambda_3 (\bar{\Psi}_D \Psi_D) (\bar{\Psi}_S \Psi_S), \end{aligned} \quad (2)$$

m_{0D}, m_{0S} are bare masses and D_μ is the covariant derivative

$$D_\mu = \partial_\mu - i\frac{g}{2}\underline{\tau} \underline{A}_\mu - i\frac{g'}{2}B_\mu, \quad (3)$$

where \underline{A}_μ, B_μ and g, g' are the usual weak gauge boson fields and couplings, respectively. The left handed and the right handed fermions are assumed to be gauged under the same gauge $SU_L(2)$ group. Additional four-fermion couplings are possible but the extra term will not fundamentally change the symmetry breaking and mass generation. We will show in what follows that for couplings λ_i exceeding the critical value the four-fermion interactions of (2) generate condensates

$$\left\langle \bar{\Psi}_{D\alpha}^0 \Psi_{D\beta}^0 \right\rangle_0 = a_1 \delta_{\alpha\beta}, \quad (4)$$

$$\left\langle \bar{\Psi}_{D\alpha}^+ \Psi_{D\beta}^+ \right\rangle_0 = a_+ \delta_{\alpha\beta}, \quad (5)$$

$$\left\langle \bar{\Psi}_{S\alpha} \Psi_{S\beta} \right\rangle_0 = a_2 \delta_{\alpha\beta}, \quad (6)$$

$$\left\langle \bar{\Psi}_S \Psi_D \right\rangle_0 = \left\langle \begin{pmatrix} \bar{\Psi}_S \Psi_D^+ \\ \bar{\Psi}_S \Psi_D^0 \end{pmatrix} \right\rangle_0 \neq 0. \quad (7)$$

The formation of the charged condensate (5) first appeared in [38] and is more general than the condensates in [26]. The non-diagonal condensate in (7) spontaneously breaks the group $SU_L(2) \times U_Y(1)$ to $U_{em}(1)$ of electromagnetism. With the gauge transformations of Ψ_D the condensate (7) can always be transformed into a real lower component,

$$\langle \bar{\Psi}_{S\alpha} \Psi_{D\beta}^0 \rangle_0 = a_3 \delta_{\alpha\beta}, \quad \langle \bar{\Psi}_{S\alpha} \Psi_{D\beta}^+ \rangle_0 = 0, \quad (8)$$

where a_3 is real. The composite operator $\bar{\Psi}_S \Psi_D$ resembles the standard scalar doublet.

Assuming invariant four-fermion interactions for the new and known fermions,

$$L_f = g_f \left(\bar{\Psi}_L^f \Psi_R^f \right) (\bar{\Psi}_S \Psi_D) + g_f \left(\bar{\Psi}_R^f \Psi_L^f \right) (\bar{\Psi}_D \Psi_S), \quad (9)$$

the condensate (8) generates masses to the standard fermions. In the linearized, mean field approximation the electron mass, for example, is

$$m_e = -4g_e a_3. \quad (10)$$

Up type quark masses can be generated via the charge conjugate field $\tilde{\Psi}_D = i\tau_2 (\Psi_D)^\dagger$. Introducing nondiagonal quark bilinears, the Kobayashi-Maskawa mechanism emerges. As in the Standard Model, from (10) we see that for two particles $m_i/m_j = g_i/g_j$, the masses are proportional to the unconstrained generalized Yukawa coefficients.

The masses of the weak gauge bosons arise from the effective interactions of the auxiliary composite $Y = 1$ scalar doublet,

$$\Phi = \begin{pmatrix} \Phi^+ \\ \Phi^0 \end{pmatrix} = \bar{\Psi}_S \Psi_D. \quad (11)$$

Φ develops a gauge invariant kinetic term in the low energy effective description

$$L_H = h (D_\mu \Phi)^\dagger (D^\mu \Phi), \quad (12)$$

where D_μ is the usual covariant derivative (3).

The coupling constant h sets the dimension of L_H , $[h] = -4$ in mass dimension, we assume $h > 0$. (12) is a non-renormalizable Lagrangian and it provides the weak gauge boson masses and some of the interactions of the new fermions with the standard gauge bosons.

The terms with Φ^0 in L_H can be written as

$$\begin{aligned} h^{-1} L_H = & \frac{g^2}{2} W_\mu^- W^{+\mu} \Phi^{0\dagger} \Phi^0 + \frac{g^2}{4 \cdot \cos^2 \theta_W} Z_\mu Z^\mu \Phi^{0\dagger} \Phi^0 + \\ & + \left[\partial^\mu \Phi^{0\dagger} \partial_\mu \Phi^0 - \frac{i}{2} \frac{g}{\cos \theta_W} (\partial^\mu \Phi^{0\dagger}) \Phi^0 Z_\mu + \frac{i}{2} \frac{g}{\cos \theta_W} \Phi^{0\dagger} Z_\mu (\partial^\mu \Phi^0) \right] \end{aligned} \quad (13)$$

in terms of the standard vector boson fields.

In the linearized approximation in (13) we put

$$h \Phi^{0\dagger} \Phi^0 \rightarrow h \langle \Phi^{0\dagger} \Phi^0 \rangle_0 = h (16a_3^2 - 4a_1a_2) = \frac{v^2}{2}, \quad (14)$$

leading to the standard masses

$$m_W = \frac{gv}{2}, \quad m_Z = \frac{gv}{2 \cos \theta_W}. \quad (15)$$

v^2 is, as usual, $(\sqrt{2}G_F)^{-1}$, $v = 254$ GeV. The tree masses naturally fulfill the important relation $\rho_{\text{tree}} = 1$. This relation is the direct consequence of the extra global (custodial) $SU(2)$ symmetry [39] of the Lagrangian (12) and of the vacuum expectation value of the composite scalar field. The complete symmetry breaking sector, the Lagrangian (2) does not show this extra global symmetry, because there are mass-like terms breaking the symmetry of global chiral rotations. However, this symmetry breaking does not influence the W^\pm, Z mass ratio. The idea is that there is a compositeness scale at the order of the cutoff Λ , where the vacuum expectation values of the new fermions and composite field Φ is formed, which decouples from the original fermions at lower energies. This way the composite scalar field Φ can have separate global custodial symmetry and the new fermions can only influence the ϱ parameter via suppressed loop corrections.

3 Gap equations

Once the condensates (4-7) are formed, dynamical mass terms are generated in the Lagrangian (2) beside the bare mass terms.

$$L_\psi \rightarrow L_\psi^{\text{lin}} = -m_+ \overline{\Psi}_D^+ \Psi_D^+ - m_1 \overline{\Psi}_D^0 \Psi_D^0 - m_2 \overline{\Psi}_S \Psi_S - m_3 \left(\overline{\Psi}_D^0 \Psi_S + \overline{\Psi}_S \Psi_D^0 \right), \quad (16)$$

with

$$m_+ = m_{0D} - 6\lambda_1 a_+ - 8(\lambda_1 a_1 + \lambda_3 a_2) = m_1 + 2\lambda_1 (a_+ - a_1) \quad (17)$$

$$m_1 = m_{0D} - 6\lambda_1 a_1 - 8(\lambda_1 a_+ + \lambda_3 a_2), \quad (18)$$

$$m_2 = m_{0S} - 6\lambda_2 a_2 - 8\lambda_3 (a_1 + a_+), \quad (19)$$

$$m_3 = 2\lambda_3 a_3. \quad (20)$$

If $m_3 = 0$ ($\lambda_3 = 0$ or $a_3 = 0$) then (16) is diagonal, the original gauge eigenstates are the physical fields, the electroweak symmetry is not broken, $\lambda_3 a_3$, the non-diagonal condensate triggers the mixing and symmetry breaking. If $m_3 \neq 0$ (16) is diagonalized via unitary transformation to get physical mass eigenstates

$$\begin{aligned} \Psi_1 &= c \Psi_D^0 + s \Psi_S, \\ \Psi_2 &= -s \Psi_D^0 + c \Psi_S, \end{aligned} \quad (21)$$

Figure 1. Feynman graphs for the gap equation (18). Similar graphs corresponding to (17,19) with exchanged legs and lines.

Figure 2. Feynman graphs for the gap equation (20).

where $c = \cos \phi$ and $s = \sin \phi$, ϕ is the mixing angle. As Ψ_S is real only the real components of Ψ_D^0 take part in the mixing. The masses of the physical fermions Ψ_1, Ψ_2 are

$$2M_{1,2} = m_1 + m_2 \pm \frac{m_1 - m_2}{\cos 2\phi}. \quad (22)$$

The mixing angle is defined by

$$2m_3 = (m_1 - m_2) \tan 2\phi. \quad (23)$$

Again we see, once $m_3 = 0$ the mixing angle vanishes (for $m_1 \neq m_2$), $M_1 = m_1$ and $M_2 = m_2$. The physical masses will be equal ($M_1 = M_2$) only if $m_1 = m_2$, the original neutral fermions are degenerate in mass and then the mixing angle is meaningless from the point of view of mass matrix diagonalization.

It follows that the physical eigenstates themselves form condensates since

$$\begin{aligned} c^2 \langle \bar{\Psi}_{1\alpha} \Psi_{1\beta} \rangle_0 + s^2 \langle \bar{\Psi}_{2\alpha} \Psi_{2\beta} \rangle_0 &= a_1 \delta_{\alpha\beta}, \\ s^2 \langle \bar{\Psi}_{1\alpha} \Psi_{1\beta} \rangle_0 + c^2 \langle \bar{\Psi}_{2\alpha} \Psi_{2\beta} \rangle_0 &= a_2 \delta_{\alpha\beta}, \\ cs \langle \bar{\Psi}_{1\alpha} \Psi_{1\beta} \rangle_0 - cs \langle \bar{\Psi}_{2\alpha} \Psi_{2\beta} \rangle_0 &= a_3 \delta_{\alpha\beta}. \end{aligned} \quad (24)$$

There is no non-diagonal condensate as Ψ_1, Ψ_2 are independent. Combining the equations of (24) one finds

$$a_3 = \frac{1}{2} \tan 2\phi (a_1 - a_2). \quad (25)$$

For $a_1 = a_2$, $a_3 \neq 0$ is not possible for $\cos 2\phi \neq 0$. As is seen, (25) is equivalent to $\langle \bar{\Psi}_{1\alpha} \Psi_{2\beta} \rangle_0 = 0$. Comparing (25) to (23) yields

$$m_1 - m_2 = 2\lambda_3 (a_1 - a_2). \quad (26)$$

Using the equations (17-20) we are lead to a consistency conditions

$$(\lambda_3 - \lambda_1) \left(a_1 + \frac{4}{3} a_+ \right) = (\lambda_3 - \lambda_2) a_2, \quad (27)$$

$\lambda_1 \neq \lambda_2$ goes with $a_1 + \frac{4}{3}a_+ \neq a_2$.

The equations (17-20) can be formulated as gap equations [32] in terms of the physical fields expressing both the masses and the condensates with Ψ_1 , Ψ_2 and $\Psi_+ \equiv \Psi_D^+$. Assuming vanishing original masses, $m_{0S} = 0$, $m_{0D} = 0$, the complete set of gap equations are

$$c \cdot s (M_1 - M_2) = 2\lambda_3 c \cdot s (I_1 - I_2), \quad (28)$$

$$c^2 M_1 + s^2 M_2 = -\lambda_1 (6(c^2 I_1 + s^2 I_2) + 8I_+) - 8\lambda_3 (s^2 I_1 + c^2 I_2), \quad (29)$$

$$s^2 M_1 + c^2 M_2 = -6\lambda_2 (s^2 I_1 + c^2 I_2) - 8\lambda_3 (c^2 I_1 + s^2 I_2 + I_+), \quad (30)$$

$$M_+ = -\lambda_1 (8(c^2 I_1 + s^2 I_2) + 6I_+) - 8\lambda_3 (s^2 I_1 + c^2 I_2). \quad (31)$$

The main task of the present work is to explore the structure of the gap equations. There are four algebraic equations for four variables M_1 , M_2 , M_+ , $c^2 = \cos^2 \phi$. As in almost all approximation $I_i \sim M_i$, (28-31) show gap equation characteristics, $M_i = 0$ is always a symmetric solution, which is stable for small $|\lambda_i|$. Increasing $|\lambda_i|$ also an energetically favoured [40] massive solution emerges as in the original Nambu Jona-Lasinio model. Now we explore the parameter space λ_i to find acceptable physical masses.

Let the condensates be approximated by free field propagators

$$\langle \bar{\Psi}_{i\alpha} \Psi_{i\beta} \rangle = \frac{\delta_{\alpha\beta}}{4} I_i = -\frac{\delta_{\alpha\beta}}{8\pi^2} M_i \left(\Lambda^2 - M_i^2 \ln \left(1 + \frac{\Lambda^2}{M_i^2} \right) \right), \quad i = 1, 2, +, \quad (32)$$

where $M_+ = m_+$. Here Λ is a four-dimensional physical cutoff, it sets the scale of the new physics responsible for the non-renormalizable operators. From the point of view of symmetry breaking, the Λ cutoff can be chosen arbitrary large (below the GUT or Planck scale), but higher Λ implies stronger fine tuning of λ_3 , see (32), to keep the new fermion masses in the electroweak range. To avoid fine tuning and allow reasonable fermion masses Λ is expected to be a few TeV, typically around 3 TeV [26].

For the electroweak symmetry breaking the most important equation is (28), it triggers mixing between the different representations of the weak gauge group. Applying (32) it reads

$$0 = (M_1 - M_2) c \cdot s \left(\frac{1}{\lambda_3} + \frac{\Lambda^2}{\pi^2} - \frac{M_1^3 \ln \left(1 + \frac{\Lambda^2}{M_1^2} \right) - M_2^3 \ln \left(1 + \frac{\Lambda^2}{M_2^2} \right)}{M_1 - M_2} \right). \quad (33)$$

(33) always has a symmetric solution $(M_1 - M_2) c \cdot s = 0$, implying $\sin 2\phi = 0$ for $M_1 \neq M_2$, there is essentially no mixing. $M_1 = M_2$ is discussed after (23). If $|\lambda_3|$ is greater than a critical value $|\lambda_3^c| = \frac{\pi^2}{\Lambda^2}$ there also exists a symmetry breaking solution ($M_1 \neq M_2$), which always has lower energy if the massive solution exists [40]. Equation (33) has a solution with moderate masses ($M_{1,2} < 0.7\Lambda$) if λ_3 is negative. In the small mass limit the parantheses in (33) simplifies to $\frac{1}{\lambda_3} + \frac{\Lambda^2}{\pi^2} - (M_1^2 + M_1 M_2 + M_2^2) \left(\ln(\Lambda^2) - \ln(\tilde{M}^2) \right)$ where $\tilde{M} \simeq \max(M_1, M_2)$. If $|\lambda_3|$ is slightly larger than its critical value, then we generally get

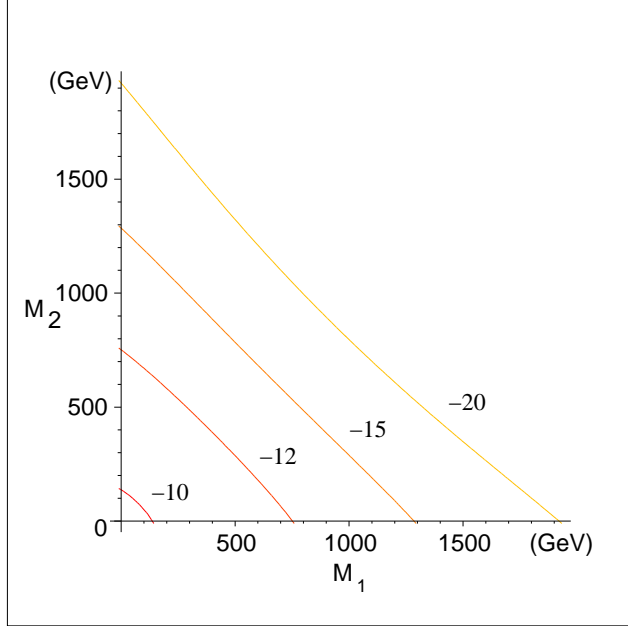


Figure 3. Constant λ_3 contours in the M_1 - M_2 plane for $\lambda_3 = \{-10, -12, -15, -20\} \cdot 1/\Lambda^2$, $\Lambda = 3$ TeV.

small masses compared to Λ , $M_1^2 + M_1 M_2 + M_2^2 \ll \Lambda^2$. The critical coupling agrees with the original Nambu-Jona Lasinio value, only a factor of two coming from the definition in the Lagrangian (2). If $|\lambda_3| < |\lambda_3^c|$ then the parantheses does not vanish in (33), the condensate a_3 is not formed and $(M_1 - M_2)c \cdot s = 0$. The physical solution is $c \cdot s = 0$, there is no meaningful mixing, Ψ_S, Ψ_D are the physical mass eigenstates, and the electroweak symmetry is not broken.

Despite the complicated structure of the non-linear equations (28-31) we get a relatively simple gap equation for λ_1 , similar to (33), from (17) $2\lambda_1(a_1 - a_+) = m_1 - m_+$. In the physical fields we have

$$M_+ - c^2 M_1 - s^2 M_2 = 2\lambda_1 (I_+ - c^2 I_1 - s^2 I_2). \quad (34)$$

It includes four unknowns, therefore it cannot be analyzed directly. We get a useful restriction solving (28) and (29) for λ_1 and substituting it to (34), relating M_1, M_2, M_+ and c^2 independently of the λ_i 's. Requiring that $0 \leq c^2 \leq 1$ we get

$$M_1 \leq M_+ \leq M_2. \quad (35)$$

As a result of the logarithmic terms in I_i , M_+ is nonlinear in c^2 , while $m_1 = c^2 M_1 + s^2 M_2$. We remark that though (28) and (34) are very similar, for moderate masses λ_3 is always negative, while λ_1 is positive (also $\lambda_2 > 0$). In the $c^2 = 0$ (1) limit $M_+ = M_2$ (M_1) and there are cancellations in (28-31). Turning back to the symmetric solution of (33) the relation (35) gives $M_+ = M_1 = M_2$ and the rest of the gap equations set the common mass equal to zero unless the special relation $6(\lambda_3 - \lambda_2) = 8(\lambda_3 - \lambda_1)$ holds to provide cancellations.

To find the critical value for λ_1 and λ_2 we considered the limit $M_+ \rightarrow M_2 = M$ and $M_1 \rightarrow 0$ then

$$\lambda_1 = \frac{1}{7} \frac{\pi^2}{\Lambda^2 - M^2 \ln\left(1 + \frac{\Lambda^2}{M^2}\right)}, \quad \lambda_2 = \frac{4}{3} \frac{\pi^2}{\Lambda^2 - M^2 \ln\left(1 + \frac{\Lambda^2}{M^2}\right)}. \quad (36)$$

We get the same NJL type expression if we take the limit $M_+ \rightarrow M_2 = M$ and $M_1 \rightarrow 0$. (36) provides massive solutions if $\lambda_1 \geq \frac{1}{7} \frac{\pi^2}{\Lambda^2}$ and $\lambda_2 \geq \frac{4}{3} \frac{\pi^2}{\Lambda^2}$. Numerical scans show that these are the minimal, critical values for the couplings and can be approximated in special limits. Numerical solutions are shown in Table 1. for cutoff $\Lambda = 3$ TeV. The role of M_1 and M_2 can be exchanged together with $c^2 \leftrightarrow s^2$, therefore we have chosen $M_1 < M_2$ without the loss of generality. As the cutoff is not too high, 3 TeV, there is no serious fine tuning in the λ_i 's to find relatively small masses.

To understand the signs and roughly the factors in $\lambda_{1,2}^c$ consider the limit $M_1 \simeq M_2 \simeq M_+ \simeq M$. If $M \ll \Lambda$ then $\lambda_3 \simeq \lambda_3^c = -\frac{\pi^2}{\Lambda^2}$, though in the exact limit (28) becomes singular. We get from (28-31) the relation $14\lambda_1 = 6\lambda_2 + 8\lambda_3$ and a single gap equation ($I = I_M$ in (32))

$$M = -(14\lambda_1 + 8\lambda_3) I. \quad (37)$$

Small mass solution requires $\tilde{\lambda} = 14\lambda_1 + 8\lambda_3$ to be close to it's critical value $2\pi^2/\Lambda^2$ and provides rough estimates $\lambda_1 \sim \frac{5}{7} \frac{\pi^2}{\Lambda^2}$ and also $\lambda_2 \sim 3 \frac{\pi^2}{\Lambda^2}$ to generate small masses. Numerical solutions also provide general (M_+ not close to M_1 or M_2) small masses for couplings close to these values, see Table 1.

$\lambda_1 \left(\frac{\pi^2}{\Lambda^2}\right)$	0.546	0.740	0.496	0.380	0.502	0.468	0.419
$\lambda_2 \left(\frac{\pi^2}{\Lambda^2}\right)$	2.540	3.11 (!)	2.403	2.120	2.457	2.455	2.451
$\lambda_3 \left(\frac{\pi^2}{\Lambda^2}\right)$	-1.031	-1.041	-1.042	-1.070	-1.083	-1.178	-1.330
M_1 (GeV)	100	148	100	100	150	200	200
M_2 (GeV)	150	150	200	300	300	500	800
M_+ (GeV)	149	149	190	290	290	490	790

Table 1: Solutions of the gap equations for the cutoff $\Lambda = 3$ TeV, λ_i are given in units of $\frac{\pi^2}{\Lambda^2}$. In the second column λ_2 violates perturbative unitarity.

In the strongest small mass limit one neglects the logarithmic terms in the condensates (32), and equations (28-31) reduce to a linear homogeneous system of equations [38]. Finally we get two relations for the masses, $M_+ = m_1 = c^2 M_1 + s^2 M_2$ and $\frac{m_1}{m_2} = \frac{1-6\lambda_2\Lambda^2/\pi^2}{16\lambda_3\Lambda^2/\pi^2} = \frac{8\lambda_3\Lambda^2/\pi^2}{1-14\lambda_1\Lambda^2/\pi^2}$.

The solutions of the gap equations are further constrained by perturbative unitarity.

4 Perturbative unitarity

In this section we apply tree-level partial wave unitarity to two-body scatterings of the new fermions following the arguments of the pioneering work by Lee et al. [41], where perturbative unitarity has been employed to constrain the Standard Model Higgs mass. Perturbative unitarity is a powerful tool, it can be used to build up the bosonic sector of the Standard Model, moreover it was essential to build higgsless models of electroweak symmetry breaking in extra dimensional field theories [25]. The method was used to constrain the parameters in the dynamical symmetry breaking vector condensate model in [42].

Consider the amplitudes of two particle $(\Psi_D^{(+)}, \Psi_D^{(0)} \text{ or } \Psi_S)$ elastic scattering processes and impose $|\Re a_0| \leq 1/2$ for the $J = 0$ partial wave amplitudes. The contact graph gives the dominant contribution, neglecting the fermion masses for the $\Psi_D^{(+)}\Psi_D^{(-)}$ scattering gives an upper bound on λ_1 coupling, $|\lambda_1| s \leq 8\pi$, where s is the maximal center of mass energy ($M_+^2 \ll s \leq \Lambda^2$).

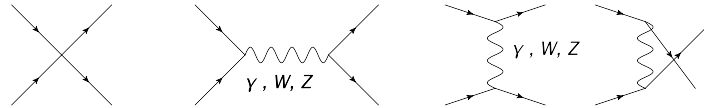


Figure 4. Feynman graphs of 2-particle elastic scattering

We cannot always use the small mass limit, as the solution of the gap equations provide higher λ_i 's for significantly higher masses. Therefore we have calculated different helicity amplitudes [43] for non-vanishing masses. For $\Psi_a(1)\bar{\Psi}_a(2) \rightarrow \Psi_a(3)\bar{\Psi}_a(4)$, ($a = 0, s, +$), $M = \lambda_i [(\bar{v}_2 u_1)(\bar{u}_3 v_4) - (\bar{u}_3 u_1)(\bar{v}_2 v_4)]$, where $\lambda_{i=1,2,3}$ are the only relevant four-fermion couplings. We consider $\Psi_S = s\Psi_1 + c\Psi_2$ scattering as a linear combination in the coupled Ψ_1, Ψ_2 channels to employ only λ_2 (and similarly $\Psi_D^{(0)}$ to constrain λ_1). The contributions of the γ, Z exchange graphs are negligible ($\mathcal{O}(g^2) \ll 8\pi$) because of the extra propagator. There are three different helicity channels, we give the representative helicity amplitudes, these are maximal for the back to back scattering ($\theta_{\text{scattering}}^{13} = \pi$)

$$M((+-) \rightarrow (+-)) = \lambda_i (s - 4M_i^2), \quad (38)$$

$$M((++) \rightarrow (--)) = \lambda_i s, \quad (39)$$

$$M((+-) \rightarrow (-+)) = \lambda_i 4M_i^2. \quad (40)$$

For other scattering angles $|M|$ is smaller than in (39), for example the maximum for $\theta = 0$ is $\lambda_i 4M_i^2$. The mass dependent unitarity bound agrees with the first estimate

$$\lambda_i s \leq 8\pi, \quad (41)$$

where $i=1,2,3$ and $s \leq \Lambda^2$ is the center of mass energy. The unitarity constraints are most stringent for λ_2 , even the equal small mass limit (37) would set $\lambda_2 \simeq 3\pi^2/\Lambda^2$ which is above the maximum value allowed by unitarity $8\pi/\Lambda^2 \simeq 2.55 \cdot \frac{\pi^2}{\Lambda^2}$. As an example we

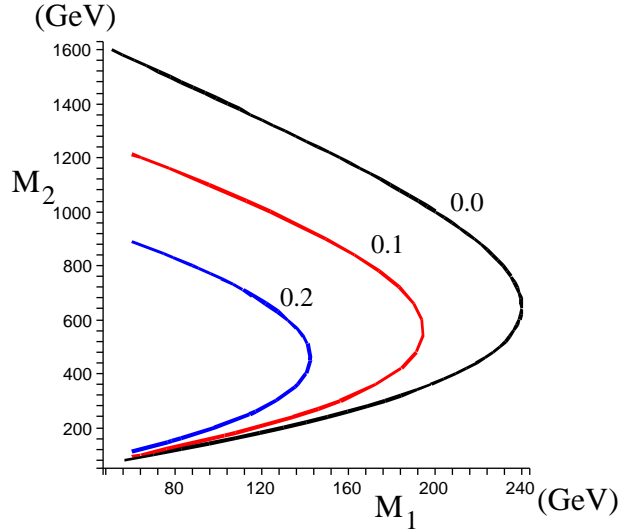


Figure 5. The maximum value of $c^2 = \cos^2 \Phi$ on the M_1, M_2 plane from the gap equation and unitarity. c^2 can be higher inside the curves.

show a non-physical nearly equal mass solution in the second column of Table 1., which is not allowed by perturbative unitarity. (41) implies an absolute upper bound on the smaller neutral mass, $M_1 < 240$ GeV for $\Lambda = 3$ TeV. Perturbative unitarity for λ_2 and the solution of the gap equations generally push up the charged mass close to M_2 and sets the mixing angle $\sin \phi$ close to 1 in (21) meaning that there is only a small mixing, Ψ_2 is mostly composed of Ψ_D^0 and there is only a small mass splitting in the doublet Ψ_D after symmetry breaking. This observation will be important to estimate electroweak oblique corrections. The allowed M_1, M_2 masses and the maximum value of c^2 is shown in Figure 5. The maximum value of the cosine of mixing angle is determined from the condition that λ_2 should stay below the unitarity bound (41). The charged fermion mass must be relatively close to the mass of the heavier neutral one. The mixing angle ϕ is relatively close to $\cos \phi \sim 0$, the mixing is weak, see the curve on the right in Figure 6. Ψ_2 is mostly composed of Ψ_D^0 and there is only a small mass splitting in the doublet Ψ_D after symmetry breaking.

5 Interactions with W^\pm, Z and constraints from the Z decay

The collider phenomenology and radiative corrections (see section 6) in the model are coming from the doublet kinetic term in (2) taking into account the mixing (21)

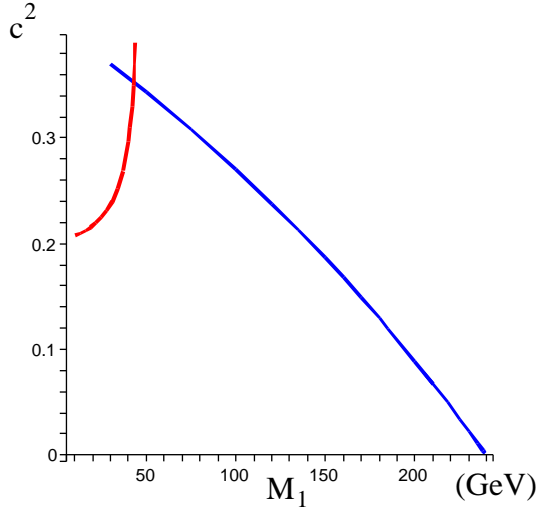


Figure 6. The maximum value of the $c^2 = \cos^2 \Phi$ vs. the lighter neutral mass M_1 . The right (blue) curve is derived from the gap equation and unitarity. The upper left (red) curve is from the width of the Z boson.

$$\begin{aligned}
L^I = & \quad \bar{\Psi}_D^+ \gamma^\mu \Psi_D^+ \left(\frac{g'}{2} B_\mu + \frac{g}{2} W_{3\mu} \right) + \\
& + \left(c^2 \bar{\Psi}_1 \gamma^\mu \Psi_1 + s^2 \bar{\Psi}_2 \gamma^\mu \Psi_2 - sc (\bar{\Psi}_1 \gamma^\mu \Psi_2 + \bar{\Psi}_2 \gamma^\mu \Psi_1) \right) \left(\frac{g'}{2} B_\mu - \frac{g}{2} W_{3\mu} \right) + \\
& + \left[\frac{g}{\sqrt{2}} W_\mu^+ \left(c \bar{\Psi}_D^+ \gamma^\mu \Psi_1 - s \bar{\Psi}_D^+ \gamma^\mu \Psi_2 \right) + h.c. \right]. \tag{42}
\end{aligned}$$

The interactions between the new and the standard fermions in L_f (9) turns out to be very weak. Indeed, from (10) and (14) we have an upper bound for g_e , $g_e \leq \sqrt{2h} \frac{m_e}{v} = \sqrt{2h} g_e^{SM}$, which is suppressed by two factors of the scale of new physics compared to the standard model value g_e^{SM} .

We will explore the consequences of these interactions in the decay of the Z boson and in the precision electroweak test of the standard model in the next section.

The proposed new fermions could not be seen in the high energy experiments so far, because of their large masses and/or small couplings to ordinary particles. The mixing in the doublet reduces the coupling to the gauge bosons, but the new charged fermion is not affected. From the LEP1 and LEP2 measurements there is lower bound for the mass of a heavy charged lepton, valid here $M_+ > 100$ GeV [1]. For the neutral component of the doublet (without mixing) there are smaller lower bounds; without further assumptions $M_2 > 45$ GeV. Using the relation (35) M_2 is at least 100 GeV with or without mixing. The mixing generates small, but non-vanishing coupling between the Z boson and the new lighter neutral fermion (e.g. the remnant of the singlet, it has c^2 part of a doublet).

Therefore if it is light enough it contributes to the invisible width of the Z boson

$$\Gamma(Z \rightarrow \bar{\Psi}_1 \Psi_1) = \frac{\sqrt{2}G_F M_Z^3}{6\pi} \left(\frac{c^4}{4}\right) \sqrt{1 - \frac{4M_1^2}{M_Z^2}}. \quad (43)$$

The Z width is experimentally known at high precision and the pull factor is rather small

$$\Gamma(Z) = (2.4952 \pm 0.0023)\text{GeV}. \quad (44)$$

We estimate the maximum possible room for new physics as 3σ in the experimental Z width, $\Gamma_Z^{\text{new}} < 7$ MeV. In [44] the minimum value of Γ_Z^{theory} (at maximum $\sin^2 \theta_W$ and minimum M_Z^2 and α_S) was compared to the maximal experimental value, and gave a similar 3σ window for new physics. We see that M_1 masses well below $M_Z/2$ are still allowed for rather small mixing, see the (red) curve on the left on Figure 6.

6 Electroweak precision parameters

The new fermions have direct interactions with the standard fermions (9) and gauge bosons (42). The four-fermion couplings of the new particles to the light fermions are weak; weaker than the corresponding ones in the Standard Model [26]. The new couplings to the gauge bosons are the gauge couplings suppressed only by the $\mathcal{O}(1)$ mixing factors. Therefore the couplings to the light fermions which participate in the precision experiments, are suppressed compared to the couplings to the gauge bosons. The new fermions thus mainly contribute to the gauge boson self energies in the precision experiments. In most of the solutions of the gap equation [38] $M_+, M_2 \gg M_Z$. Expecting further $M_1 > M_Z$ we can give a good estimate of the effects of new physics in terms of the general S, T and U parameters introduced by Peskin and Takeuchi [35]. We get a rough estimate of the loop effects if the mass of the lighter neutral fermion is not far above the Z mass.

The two relevant parameters, S and T defined via the gauge boson self energies

$$\alpha(M_Z) T = \frac{\Pi_{WW}^{\text{new}}(0)}{M_W^2} - \frac{\Pi_{ZZ}^{\text{new}}(0)}{M_Z^2}, \quad (45)$$

$$\frac{\alpha(M_Z)}{4s_W^2 c_W^2} S = \frac{\Pi_{ZZ}^{\text{new}}(M_Z^2) - \Pi_{ZZ}^{\text{new}}(0)}{M_Z^2} - \frac{c_W^2 - s_W^2}{c_W s_W} \frac{\Pi_{Z\gamma}^{\text{new}}(M_Z^2)}{M_Z^2} - \frac{\Pi_{\gamma\gamma}^{\text{new}}(M_Z^2)}{M_Z^2}, \quad (46)$$

where $s_W^2 = \sin^2 \theta_W(M_Z)$ and $c_W^2 = \cos^2 \theta_W(M_Z)$ are \sin^2 (\cos^2) of the weak mixing angle. Barbieri et al. [45] revised the definition of the oblique parameters. The Π functions are defined from the transverse gauge boson vacuum polarization amplitudes expanded around zero $\Pi_{ab}(q^2) \simeq \Pi_{ab}(0) + q^2 \Pi'_{ab}(0) + 1/2 \cdot q^2 \Pi''_{ab}(0) + \dots$, (a,b = 1,3,Y) up to second order. The 12 coefficients define 7 parameter at the end. The definitions of the old parameters

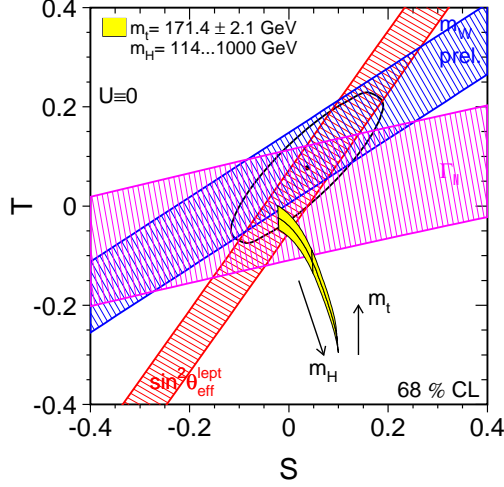


Figure 7. Experimental constraints and Standard Model predictions for S and T [46].

are

$$\frac{\alpha(M_Z)}{4s_W^2 c_W^2} S = \Pi'_{3Y}{}^{\text{new}}(0) \quad (47)$$

$$\alpha(M_Z) T = \frac{1}{M_W^2} (\Pi'_{33}{}^{\text{new}}(0) - \Pi'_{11}{}^{\text{new}}(0)), \quad (48)$$

$$\frac{\alpha(M_Z)}{4s_W^2} U = \Pi'_{33}{}^{\text{new}}(0) - \Pi'_{11}{}^{\text{new}}(0). \quad (49)$$

These parameters (with the extra 4 $-V, X, Y$ and W) fall into three groups according to their symmetry properties [45]. The Peskin-Takeuchi S parameter is custodially symmetric but weak isospin breaking. The T and U parameters break both the custodial and the weak isospin symmetry. It is reasonable to expect (and the actual calculation justifies the assumption) that the parameters with the same symmetry properties are related to each other. Since U mainly differs from T by an extra derivation of the Π functions, $U \sim \frac{M_W^2}{M_{\text{new}}^2} T$ is expected, where M_{new} is the mass scale of new physics. When there is a gap between M_{new} and M_W it is reasonable to keep only the lowest derivative terms with a given symmetry property, S and T . If there is no special fine tuning U is expected to be less important than T and S is kept as the leading effect in its symmetry class.

The experimental data determines S, T and U [1]

$$S = -0.10 \pm 0.10 \text{ } (-0.08), \quad (50)$$

$$T = -0.08 \pm 0.11 \text{ } (+0.09), \quad (51)$$

$$U = +0.15 \pm 0.11 \text{ } (+0.01), \quad (52)$$

where the central value assumes $M_H = 117$ GeV and in parentheses. The difference is shown for $M_H = 300$ GeV. The various experimental constraints and the dependence on

the top and Higgs mass can be seen in Figure 7. In our model the Higgs mass of the fit is understood as the contribution of a composite Higgs particle with the given mass.

The contributions of the new sector to the gauge boson vacuum polarizations are fermion loops with generally two non-degenerate masses m_a and m_b [48]. In the low energy effective model we have performed the calculation with a 4-dimensional Euclidean momentum cutoff Λ . The coupling constants are defined in the usual manner $L^I \sim V_\mu \bar{\Psi} (g_V \gamma^\mu + g_A \gamma_5 \gamma^\mu) \Psi$

$$\Pi(q^2) = \frac{1}{4\pi^2} \left(g_V^2 \tilde{\Pi}_V + g_A^2 \tilde{\Pi}_A \right). \quad (53)$$

The electroweak parameters depend on the values and derivatives of the Π functions at $q^2 = 0$

$$\begin{aligned} \tilde{\Pi}_V(0) = & \frac{1}{4}(m_a^2 + m_b^2) - \frac{1}{2}(m_a - m_b)^2 \ln \left(\frac{\Lambda^2}{m_a m_b} \right) - \\ & - \frac{m_a^4 + m_b^4 - 2m_a m_b (m_a^2 + m_b^2)}{4(m_a^2 - m_b^2)} \ln \left(\frac{m_b^2}{m_a^2} \right). \end{aligned} \quad (54)$$

The first derivative is

$$\begin{aligned} \tilde{\Pi}'_V(0) = & -\frac{2}{9} - \frac{4m_a^2 m_b^2 - 3m_a m_b (m_a^2 + m_b^2)}{6(m_a^2 - m_b^2)^2} + \frac{1}{3} \ln \left(\frac{\Lambda^2}{m_a m_b} \right) + \\ & + \frac{(m_a^2 + m_b^2)(m_a^4 - 4m_a^2 m_b^2 + m_b^4) + 6m_a^3 m_b^3}{6(m_a^2 - m_b^2)^3} \ln \left(\frac{m_b^2}{m_a^2} \right). \end{aligned} \quad (55)$$

For completeness we give the second derivative, too. It can be used to calculate further precision parameters [45, 47] e.g. extra two parameters introduced by Barbieri et al., and it is presented for extra vector-like fermions in [49],

$$\tilde{\Pi}''_V(0) = \frac{(m_a^2 + m_b^2)(m_a^4 - 8m_a^2 m_b^2 + m_b^4)}{8(m_a^2 - m_b^2)^4} + \frac{m_a m_b (m_a^4 + 10m_a^2 m_b^2 + m_b^4)}{6(m_a^2 - m_b^2)^4} - \quad (56)$$

$$- \frac{m_a^3 m_b^3 (3m_a m_b - 2m_a^2 - 2m_b^2)}{2(m_a^2 - m_b^2)^5} \ln \left(\frac{m_b^2}{m_a^2} \right). \quad (57)$$

We get the functions for axial vector coupling by flipping exactly one of the masses in the previous results ($m_a \rightarrow m_a$ and $m_b \rightarrow -m_b$). The method of our calculation has nice properties: it has no quadratic divergence as expected; it fulfills gauge invariance in two aspects, $\Pi_V(m_a, m_a, 0) = 0$ and the complete Π function is transverse, the coefficients of the $g_{\mu\nu}$ and $-p_\mu p_\nu / p^2$ parts are equal.

The values of the vacuum polarizations for identical masses ($m_b = m_a$) are smooth limits and agree with direct calculation.

$$\tilde{\Pi}_V(0) = 0, \quad \tilde{\Pi}'_V(0) = -\frac{1}{3} + \frac{1}{3} \ln \left(\frac{\Lambda^2}{m_a^2} \right), \quad \tilde{\Pi}''_V(0) = \frac{2}{15} \frac{1}{m_a^2}. \quad (58)$$

The S parameter is then given by (for the sake of simplicity the index V is omitted)

$$S = \frac{1}{\pi} \left(+\tilde{\Pi}'(M_+, M_+, 0) - c^4 \tilde{\Pi}'(M_1, M_1, 0) - s^4 \tilde{\Pi}'(M_2, M_2, 0) - 2s^2 c^2 \tilde{\Pi}'(M_2, M_1, 0) \right). \quad (59)$$

The first three terms cancel the divergent contribution of the last one.

The T parameter related to $\Delta\rho$ is

$$T = \frac{1}{4\pi s_W^2 M_W^2} \left[+\tilde{\Pi}(M_+, M_+, 0) + c^4 \tilde{\Pi}(M_1, M_1, 0) + s^4 \tilde{\Pi}(M_2, M_2, 0) + \right. \\ \left. + 2s^2 c^2 \tilde{\Pi}(M_2, M_1, 0) - 2c^2 \tilde{\Pi}(M_+, M_1, 0) - 2s^2 \tilde{\Pi}(M_+, M_2, 0) \right]. \quad (60)$$

For completeness we give the U parameter in the model

$$U = - \frac{1}{\pi} \left[+\tilde{\Pi}'(M_+, M_+, 0) + c^4 \tilde{\Pi}'(M_1, M_1, 0) + s^4 \tilde{\Pi}'(M_2, M_2, 0) + \right. \\ \left. + 2s^2 c^2 \tilde{\Pi}'(M_2, M_1, 0) - 2c^2 \tilde{\Pi}'(M_+, M_1, 0) - 2s^2 \tilde{\Pi}'(M_+, M_2, 0) \right]. \quad (61)$$

The gauge boson self-energies are calculated from a renormalizable part of a non-renormalizable theory, hence dimensional regularization can be used to calculate the general vacuum polarization function with two fermions of different masses circulating in the loop [49, 50].

7 Numerical constraints from precision tests

There are 3 free parameter in the model to confront with experiment. These can be chosen the three dimensionful four-fermion couplings $\lambda_{1,2,3}$, or more practically the two physical neutral masses M_1 , M_2 and the mixing angle, $c^2 = \cos^2 \phi$. For the cutoff $\Lambda \simeq 3$ TeV there is a maximum value for the masses, $M_1 \leq 240$ GeV. c^2 has an upper bound depending on the mass M_1 , see Figure 5. The mass of the charged fermion is given by the solution of the gap equations, the value of M_+ is close to, but not equal to $c^2 M_1 + s^2 M_2$.

If there is no real mixing $c^2 = 0$; or if $M_1 = M_2 = M_+$, then there is one degenerate vector-like fermion doublet and a decoupled singlet, and S and T vanish explicitly. In this case the new sector does not violate $SU_L(2)$ and there is an exact custodial symmetry. Increasing the mass difference in the remnants of the original doublet by increasing the $|M_1 - M_2|$ mass difference and/or moving away from the non-mixing case $c^2 = 0$, we get a higher S and T . For small violation of the symmetries S and T are expected to be small. Numerical evaluation shows that for the new masses in the range allowed by the LEP bound, gap equations and unitarity the U parameter is indeed an order of magnitude smaller than the T parameter and generally smaller than S . U is always in the experimental window. In case of relatively small masses the oblique parameters are understood as rough estimates, but still in agreement with experiment.

Generally the S parameter depends only on the masses of the new particles and the mixing angle. For the solutions of the gap equations fulfilling perturbative unitarity the S

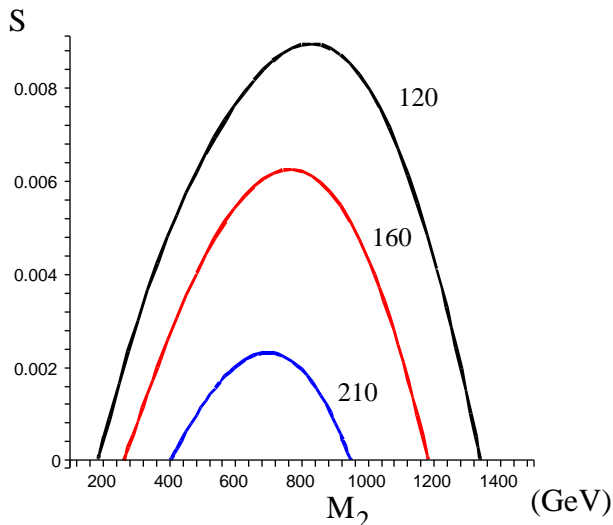


Figure 8. The maximum value of the S parameter vs. M_2 for $M_1 = 120, 160, 210$ GeV. The 95 % C.L. bounds $[-0.296, 0.096]$ are outside the figure.

parameter is always positive and far below the 95 % C.L. For a given M_1 , M_2 S increases with increasing c^2 and maximal for the highest c^2 . This maximum value of the S parameter is plotted against M_2 for three given M_1 in Figure 8. The small value of S does not constrain the parameters of the model.

The value of the T parameter is always positive. The T parameter (60) sensitive to the differences and ratios of the masses $M_{1,2,+}$. T still varies for a given (M_1, M_2) pair depending on M_+ or equally on c^2 ; T is maximal for largest mass difference, for the largest c^2 allowed by the gap equations and perturbative unitarity. The T parameter can always be in agreement with experiment for any (M_1, M_2) pair for small mixing, for $c^2 = 0$ the T parameter vanishes identically. We plotted the worst case in the (M_1, M_2) plane, the possible maximum value of the T parameter; it is given by the maximum $M_2 - M_+$ mass difference or equally for maximal c^2 .

If the Higgs is heavy, e.g. $M_H = 300$ GeV (50, 51) the central value of S decreases and T increases compared to the light Higgs case. The S parameter still in agreement with the predictions of the model. Increasing the Higgs mass the Standard Model moves away in the (S, T) plane from the experimentally allowed ellipse, see [46]. The negative contribution $(-.09)$ of the heavy Higgs to the T parameter can be compensated by the positive T contribution of the new fermions with considerable mass difference. For example (160, 800) GeV and the largest mixing $c^2 \sim 0.115$ allowed by the gap equations and unitarity gives $\Delta T \simeq 0.1$. Even heavier Higgs boson can be compensated as can be read off from Figure 9. Non-degenerate vector-like fermions with reasonable mixing allow a space for heavy Higgs in the precision tests of the Standard Model.

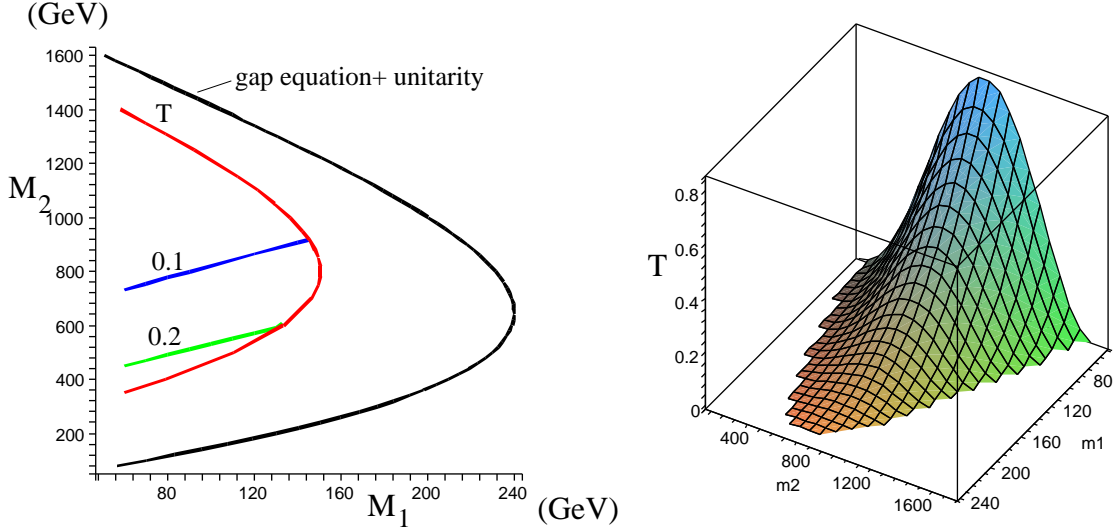


Figure 9. Constraints on the (M_1, M_2) plane. The solution of the gap equations respecting perturbative unitarity are inside the outer curve. The inner curve shows the region, where the T parameter gives the maximum value of c^2 at 95 % C.L.. Below the 0.1 (blue) and 0.2 (green) line c^2 can exceed 0.1 and 0.2. The right panel shows the maximum value of T vs. (M_1, M_2) .

8 Collider signatures

In this section we study the production of the new fermions at LHC and the planned linear collider. We focus on the production of the new charged fermions with mass M_+ , we denote it by D^+ and its antiparticle by D^- .

Since the light standard fermions are coupled very weakly to the new fermions producing pairs of new fermions is expected to be more considerable from virtual γ and Z exchanges, that is we consider the Drell-Yan mechanism, $p(\bar{p}) \rightarrow D^+D^- + X$ via quark-antiquark annihilation. The new fermion can only be produced in pairs because of the Z_2 symmetry of the original Lagrangian 2.

The Drell-Yan cross section for the above hadronic collisions can be written as

$$\sigma(p(\bar{p}) \rightarrow D^+D^- + X) = \int_{\tau_0}^1 d\tau \int_{\tau}^1 \frac{dx}{2x} \sum_i \sigma(q_i\bar{q}_i \rightarrow D^+D^-) \cdot (f_i^1(x, \hat{s})f_i^2(\tau/x, \hat{s}) + f_i^1(\tau/x, \hat{s})f_i^2(x, \hat{s})), \quad (62)$$

where x and τ/x are the parton momentum fractions, $\hat{s} = \tau s$ is the square of the centre of mass energy of $q_i\bar{q}_i$, s is the same for the hadronic initial state, $f_i^1(x, \hat{s})$ means the number distribution of i quarks in hadron 1 at the scale \hat{s} and the sum runs over the quark flavours u, d, s, c . In the computation the MSTW parton distribution functions [51] were used.

The angle integrated, colour averaged annihilation cross section $\sigma(q_i\bar{q}_i \rightarrow D^+D^-)$ is calculated at the lowest order in the gauge couplings, and QCD corrections are neglected. We hope this approximation shows the order of magnitude of the cross section. We give

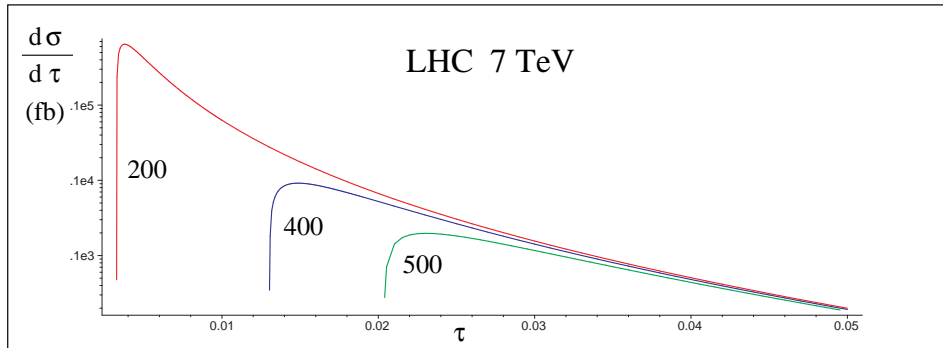


Figure 10. The differential Drell-Yan production cross section of $\Psi_D^- \Psi_D^+$ at the 7 TeV LHC.

the result of the charged final state as there is no unknown mixing angle in the estimates. The $D^+ D^-$ pairs appear via $\gamma + Z$ exchange, the relevant interactions are in (2). The cross section at the parton level is similar to the $\sigma(q_i \bar{q}_i \rightarrow \mu^+ \mu^-)$ cross section with increased masses (case of fourth family lepton), see Figure 10.

The total cross sections for different masses are shown in Table 2, and the expected number of events are very low at the delivered integrated luminosity 35 pb^{-1} .

M_+ (GeV)	200	400	500
σ (fb)	215	9.3	2.6

Table 2: Total production Drell-Yan cross section of $D^+ D^-$ at the 7 TeV LHC.

The new charged fermion D^+ may leave a charged track or a misplaced vertex if it decays in a very short time to the lighter neutral new fermion Ψ_1 . Finally the lighter neutral fermion expected to disappear leaving back missing energy and momentum, making it difficult to select this model from other sources of dark matter candidates. If new vector-like fermions can mix with the standard fermions and decay to standard particles one can search the new particles in jetmass distributions [52] and can cope with the huge background. We expect a higher yield at the 10-14 TeV LHC with the high design luminosity.

A cleaner signal is expected at the next generation of linear collider. To test the model at the forthcoming accelerators we consider the productions of new fermion pairs in electron-positron annihilation. It is most useful to investigate the case of a charged new fermion pair, we denote this $D^+ D^-$.

The contact graph from (10) yields the cross section

$$\sigma(e^+ e^- \rightarrow D^+ D^-) = \frac{g_e^2}{16\pi} s \sqrt{1 - 4 \frac{m_+^2}{s}} \left(1 - \frac{5 m_+^2}{2 s} \right), \quad (63)$$

where s is the centre of mass energy squared. The cross section is negligible at moderate s . For example at $h \sim (2 \text{ TeV})^{-4}$, $\sqrt{s} = 1 \text{ TeV}$ it is still at the order of 10^{-13} fb .

We expect a higher number of events from the photon and Z exchange processes $e^+ e^- \rightarrow$

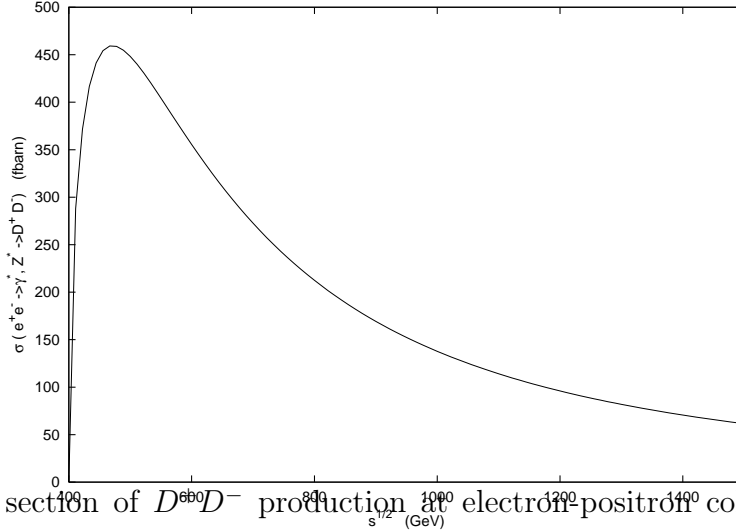


Figure 11. Cross section of D^+D^- production at electron-positron collider vs. \sqrt{s} for $m_+ = 200\text{GeV}$

$\gamma, Z \rightarrow D^+D^-$. The usual Standard Model coupling at the e^+e^-Z vertex is

$$i\frac{g}{2\cos\theta_W}\gamma_\mu(g_V + \gamma_5 g_A), \text{ where } g_V = -\frac{1}{2} + 2\sin^2\theta_W, g_A = -\frac{1}{2}.$$

By making use of (42) one obtains the cross section

$$\begin{aligned} \sigma(e^+e^- \rightarrow D^+D^-) &= \frac{1}{16\pi}\sqrt{1 - 4\frac{m_+^2}{s}}\frac{1}{s}|M|^2, \\ |M|^2 &= \frac{4}{3}e^4\frac{s + 2m_+^2}{s} + \frac{2}{3}\frac{e^4}{\sin^2\theta_W\cos^2\theta_W}g_V\frac{s + 2m_+^2}{s - m_Z^2} + \\ &+ \frac{1}{12}\frac{e^4}{\sin^4\theta_W\cos^4\theta_W}(g_V^2 + g_A^2)s\frac{s + 2m_+^2}{(s - m_Z^2)^2}, \end{aligned} \quad (64)$$

where the three terms in $|M|^2$ are coming from photon exchange, photon-Z interference and pure Z exchange. Similar cross section belongs to the neutral pair productions, too. The cross section rises fast after the threshold, at high energies it falls off as $1/s$ reflecting that all the interactions are renormalizable in the process. The cross section is given in

m_+ (GeV)	100	150	200
$\sigma(e^+e^- \rightarrow D^+D^-)$ (fb)	560	535	450

Table 3: Cross section of D^+D^- production at $\sqrt{s} = 500$ GeV

Table 3. for a few masses and plotted versus \sqrt{s} in Fig. 11. for $M_+ = 200$ GeV. At a

m_+ (GeV)	100	200	400	700
$\sigma(e^+e^- \rightarrow D^+D^-)$ (fb)	62	61	60	32

Table 4: Cross section of D^+D^- production at $\sqrt{s}=1500$ GeV

linear collider of $\sqrt{s} = 500\text{GeV}$ (TESLA) and integrated luminosity $50 \text{ fb}^{-1}/\text{year}$ a large number of events is expected.

The cross section at $\sqrt{s} = 1500\text{GeV}$ is an order of magnitude smaller but with an integrated luminosity of 100 fb^{-1} per annum a large number of events appears and higher mass range can be searched for.

9 Conclusion

In this chapter we have investigated a new dynamical symmetry breaking model of the electroweak symmetry based on four-fermion interactions of new hypothetical doublet and singlet vector-like fermions. Four-fermion interactions are postulated involving the fermions and the standard and new fermions. Gap equations were derived and we have found the conditions for dynamical symmetry breaking, in the vacuum non-diagonal condensates are formed. The lightest new particle is neutral and perturbative unitarity sets an upper bound for its mass depending on the cutoff. This particle is an ideal dark matter candidate. In the low energy effective theory limit the Higgs is a composite particle. The S and T oblique parameters were calculated and presented. The solutions of the gap equations provide masses that are always in the experimental window of the S parameter. The T parameter measures the deviation from custodial symmetry. The experimental data gives an upper bound for the mixing angle, but there is always a room for this type of new physics. This alternative of the Standard Model nicely accommodates a composite heavy Higgs in the precision electroweak test of the Standard Model. The vector-like quarks can easily compensate the negative contribution of a heavy Higgs invalidating the light Higgs preference of the present precision tests. We have presented the Drell-Yan cross section for the production of the new charged fermion at the 7 TeV LHC, the expected number of events is rather small with the 35 pb^{-1} luminosity delivered in 2010. The cross sections for linear electron-positron colliders are higher and are more promising for a potential discovery. Vector-like fermions appear in several researches beyond the Standard Model physics and can elegantly accommodate a heavy Standard Model like Higgs and provide a competitive dark matter candidate.

ACKNOWLEDGEMENT

The authors dedicate this chapter to the late George Pócsik for collaboration on the early phases of this work.

Appendix A. Regularization with momentum cutoff

There are low energy theories, like the fermion condensate model, which have an intrinsic cutoff, i.e. the upper bound of the model. The naive calculation of divergent Feynman graphs with a momentum cutoff is thought to break continuous symmetries of the model. In this case the gauge invariance of the two point function with two different fermion masses in the loops can be reconstructed by subtractions leading to finite ambiguity. To avoid these problems we used dimensional regularization in $d = 4 - 2\epsilon$ and identified the poles at $d = 2$ with quadratic divergencies while the poles at $d = 4$ with logarithmic divergencies [53]. Carefully calculating the one and two point Passarino-Veltman functions in the two schemes the divergencies are the following in the momentum cutoff regularization

$$4\pi\mu^2 \left(\frac{1}{\epsilon - 1} + 1 \right) = \Lambda^2, \quad (65)$$

$$\frac{1}{\epsilon} - \gamma_E + \ln(4\pi\mu^2) + 1 = \ln\Lambda^2, \quad (66)$$

where μ is the mass-scale of dimensional regularization. The finite part of a divergent quantity is defined by

$$f_{\text{finite}} = \lim_{\epsilon \rightarrow 0} \left[f(\epsilon) - R(1) \left(\frac{1}{\epsilon - 1} + 1 \right) - R(0) \left(\frac{1}{\epsilon} - \gamma_E + \ln 4\pi + 1 \right) \right], \quad (67)$$

where $R(1)$, are the residues of the poles at $\epsilon = 1, 0$ respectively.

We have found that contrary to the expectations the ambiguity of the cutoff regularization scheme is coming from the replacement of

$$l_\mu l_\nu \rightarrow g_{\mu\nu} l^2 / 4 \quad (68)$$

and not from shifting the loop-momentum (l).

In [54] we have worked out a symmetry preserving regularization in four dimensions. The key point is that tracing and divergent integration are not commutative. Under divergent integrals regulated by momentum cutoff in the new method the following identification will respect gauge and Lorentz symmetry during the calculation

$$\int_{\Lambda \text{ reg}} d^4 l_E \frac{l_{E\mu} l_{E\nu}}{(l_E^2 + m^2)^{n+1}} := \frac{1}{2n} g_{\mu\nu}^{(E)} \int_{\Lambda \text{ reg}} d^4 l_E \frac{1}{(l_E^2 + m^2)^n}, \quad n = 1, 2, \dots \quad (69)$$

This identification is Lorentz invariant, in gauge theories (69) guarantees the validity of the Slavnov-Taylor identities. It is shown in [55] that the ABJ triangle anomaly can be correctly calculated with this regularization.

References

- [1] K. Nakamura *et al* (Particle Data Group) 2010 J. Phys. G.: Nucl. Part. Phys. **37** 0075021 .

- [2] CDF and D0 Collaboration, Phys. Rev. Lett. 104 (2010) 061802, updated in arXiv:1007.4587 [hep-ex].
- [3] M. Goebel, PoS **ICHEP2010** (2010) 570, arXiv:1012.1331 [hep-ph].
- [4] S.Weinberg, Phy. Rev. D **13**, 974 (1976).
- [5] S.Weinberg, Phy. Rev. D **19**, 1277 (1979).
- [6] L.Susskind, Phy. Rev. D 20, 2619 (1979).
- [7] C. T. Hill and E. H. Simmons, Phys. Rept. **381** (2003) 235, [Erratum-ibid. **390** (2004) 553].
- [8] E. Eichten and K. D. Lane, Phys. Lett. B **90** (1980) 125.
- [9] S. Dimopoulos and L. Susskind, Nucl. Phys. B **155** (1979) 237.
- [10] B. Holdom, Phys. Rev. D **24** (1981) 1441.
- [11] K. Yamawaki, M. Bando and K. Matumoto, Phys. Rev. Lett. **56** (1986) 1335.
- [12] T. Appelquist, G. T. Fleming and E. T. Neil, Phys. Rev. Lett. **100** (2008) 171607.
- [13] F. Sannino and K. Tuominen, Phys. Rev. D **71** (2005) 051901.
- [14] W. A. Bardeen, C.T. Hill and M. Lindner, Phys.Rev. D **41** 1647 (1990).
- [15] C.T. Hill, Phys.Lett. **B266**, 419 (1991).
- [16] H. C. Cheng, B. A. Dobrescu and C. T. Hill, Nucl. Phys. B **589** (2000) 249.
- [17] Y. Bai, M. Carena and E. Ponton, Phys. Rev. D **81** (2010) 065004.
- [18] N. Arkani-Hamed, A.G. Cohen and H. Georgi, Phys.Lett. **B513**, 232 (2001).
- [19] L. Giusti, A. Romanino and A. Strumia, Nucl. Phys. B **550** (1999) 3.
- [20] N. Arkani-Hamed, A.G. Cohen, T. Gregoire and J.G. Wacker, JHEP **0208**, 020 (2002).
- [21] N. Arkani-Hamed, A.G. Cohen, E. Katz, A.E. Nelson, T. Gregoire, Jay G. Wacker, JHEP **0208**, 021 (2002).
- [22] H. Georgi and D. Pais, Phys. Rev. **D10** 539 (1974), ibid **D12** 508 (1975).
- [23] D. B. Kaplan, H. Georgi and S. Dimopoulos, Phys. Lett. B **136**, 187 (1984).
- [24] K. Agashe, R. Contino and A. Pomarol, Nucl. Phys. B **719** (2005) 165.

- [25] C. Csaki, C. Grojean, H. Murayama, L. Pilo and J. Terning, . *Phys. Rev. D* **46**, (1992) 381.
- [26] G. Cynolter, E. Lendvai and G. Pócsik, *Eur. Phys. J.* **C46**: 545 (2006).
- [27] T. Appelquist, H-C. Cheng, B. A. Dobrescu, *Phys. Rev. D* **64** (2001) 035002.
- [28] Riccardo Barbieri, Lawrence J. Hall, Vyacheslav S. Rychkov, *Phys. Rev. D* **74**: 015007 (2006).
- [29] R. Enberg, P.J. Fox, L.J. Hall, A.Y. Papaioannou, M. Papucci, *JHEP* **0711**: 014 (2007); Rakhi Mahbubani, Leonardo Senatore, *Phys. Rev. D* **73**: 043510 (2006).
- [30] F. D'Eramo, *Phys.Rev.D*76:083522 (2007).
- [31] W.A. Bardeen, C.T. Hill and M. Lindner, *Phys.Rev. D* **41** 1647 (1990); C.T. Hill, *Phys.Lett. B* **266**, 419 (1991); M. Lindner and D. Ross, *Nucl.Phys. B* **370**, 30 (1992); Bogdan A. Dobrescu and Christopher T. Hill, *Phys. Rev. Lett.* **81**, 2634 (1998).
- [32] Y. Nambu and G. Jona-Lasinio, *Phys. Rev.* **122**, 345 (1961); Y. Nambu and G. Jona-Lasinio, *Phys. Rev.* **124**, 246 (1961).
- [33] G. Cynolter, E. Lendvai and G. Pócsik, *Eur. Phys. J.* **C38**, 247 (2004).
- [34] G. Cynolter, E. Lendvai and G. Pocsik, arXiv:hep-ph/0412285; C. P. Hays, L. Bruchers, R. Santos, A. Gutierrez-Rodriguez, M. S. Berger, G. Cynolter and H. N. Long, "Search for the Higgs Boson," ISBN 1-59454-861-7, 2006.
- [35] M. E. Peskin and T. Takeuchi, *Phys. Rev. D* **46**, 381 (1992).
- [36] N. Maekawa, *Phys. Rev. D* **52** (1995) 1684.
- [37] N. Maekawa, *Prog. Theor. Phys.* **93** (1995) 919.
- [38] G. Cynolter and E. Lendvai, *J. Phys G* **34**, 1711 (2007).
- [39] P. Sikivie *et al.*, *Nucl. Phys. B* **173** 189, (1980).
- [40] S. P. Klevansky, *Rev. Mod. Phys.* **64**, No. 3 (1992).
- [41] B.Lee, C.Quigg and H.Thacker, *Phys. Rev. D* **16**, 1519 (1977); D.Dicus and V.Mathur, *Phys. Rev. D* **7**, 3111 (1973).
- [42] G. Cynolter, A. Bodor and G. Pocsik, *Heavy Ion Phys.* **7**, 245 (1998).
- [43] T. Appelquist, Michael S. Chanowitz, *Phys. Rev. Lett.* **59**, 2405 (1987), Erratum-ibid. **60**,1589 (1988).
- [44] G. Pócsik, E. Lendvai and G. Cynolter, *Acta Phys. Polon. B* **24** (1993) 1495.

- [45] R. Barbieri, A. Pomarol, R. Rattazzi and A. Strumia, Nucl. Phys. B**703**, 127 (2004).
- [46] LEP Electroweak Working Group homepage, <http://lepewwg.web.cern.ch/LEPEWWG>.
- [47] I. Maksymyk, C.P. Burgess and David London, Phys.Rev. D**50**, 529 (1994); G. Altarelli, R. Barbieri and S. Jadach, Nucl. Phys. B**369** 3 (1992).
- [48] G. Cynolter, E. Lendvai and G. Pócsik, Mod. Phys. Lett. A **24** (2009) 2331.
- [49] G. Cynolter and E. Lendvai, Eur. Phys. J. C **58**, 463 (2008).
- [50] L. Lavoura and J. P. Silva, Phys. Rev. D**47**, 2046 (1993).
- [51] A. D. Martin, W. J. Stirling, R. S. Thorne and G. Watt, Eur. Phys. J. C **63** (2009) 189.
- [52] Witold Skiba and David Tucker-Smith, Phys.Rev. D**75**:115010 (2007).
- [53] K. Hagiwara, S. Ishihara, R. Szalapski and D. Zeppenfeld, Phys. Rev. D **48** (1993) 2182.
- [54] G. Cynolter and E. Lendvai, arXiv:1002.4490 [hep-ph].
- [55] G. Cynolter and E. Lendvai, arXiv:1012.4648 [hep-ph].